Reports

The Rotation Period of Saturn's Polar Hexagon

D. A. Godfrey

The rotation rates of the interiors of the outer planets are normally derived from their periodic radio emissions. However, recent observations of both Jupiter and Saturn have revealed surface features with periods close to those derived for the interiors. In the study reported here, this process is carried one stage further, with the derivation of a rotation rate for the spot associated with Saturn's polar hexagon, which is simultaneously within and more accurate than the Saturnian radio period.

The hexagonal feature around Saturn's north pole was first reported by Godfrey (*1*), who noted its unusually low velocity (0.8 ± 1.1 m s^{-1}) relative to the radio rotation period. In this report I derive, using a different technique and an additional image from the Voyager 1 spacecraft, a new estimate of the velocity, with errors less than 1% of those given previously. I believe that the size and accuracy of this value (which still lies within the error bars of the radio rotation rate) make the "coincidence" hypothesis suggested in (*1*) extremely unlikely and that the burden of proof now lies with those who believe that this feature [and possibly also those reported in (*2*) and (*3*)] cannot be associated with the planet's interior. Possible causes of such a link are discussed further in (*1*) and (*2*).

Figure 1 shows a sequence of identical, polar orthographic projections of images of one quadrant of the hexagonal feature, which contains an associated larger spot. Figure 1A is from the Voyager 1 spacecraft; images B through G were returned more than 270 days later by Voyager 2. Because the spot appears to be associated with the hexagonal pattern (*1*) and to move with it (see Fig. 1), I assume that the velocity of the hexagon is the same as that of the spot.

In order to calculate the rotation rate of the larger spot, a visual estimate of its angle from the meridian (vertically up in Fig. 1) was required. I estimated the position of the center of the feature by making direct measurements (λ_c) and by averaging its eastward and westward limits [$\lambda_c' = (\lambda_e + \lambda_w)/2$]. All the measurements were repeated three times, which gave a standard error of $\approx 0.3°$. The resulting longitudes are listed as a function of time in Table 1, and the values for λ_c are shown in Fig. 2. A straight line fitted through these points, with the standard errors being estimated from the fits, gave a rotation rate of $-8.13 \pm 0.6 \times 10^{-9}$ rad s^{-1}.

National Optical Astronomy Observatories, Post Office Box 26732, Tucson, AZ 85726.

Examination of Fig. 2 leads to two obvious questions: Why was a straight line fitted, and, Since it dominates the slope, is the first point justifiable?

One can answer the second of these questions by comparing Fig. 1A with Fig 1, B through G. It is clear from this comparison that some angular motion has occurred, so that the offset between the first point and the others is significant. It should also be emphasized that the error bars shown in Fig. 2 give the repeatability of making a particular measurement of the center position. This is clearly unrelated to the systematic error associated with estimating the position of the center in different images. I believe that it is the variation in this estimation caused by the differing image illumination geometries and resolutions, and the presence of navigation errors, that produces the large errors shown in Fig. 2.

The effect of navigation errors can be roughly estimated from figure 5, a and b, in (*1*). The navigation error produces zonal velocity shifts of about 3 m s^{-1}. If the images were separated by one rotation, this would correspond to a position offset of about 0.6°. This is consistent with the scatter of the points in Fig. 2.

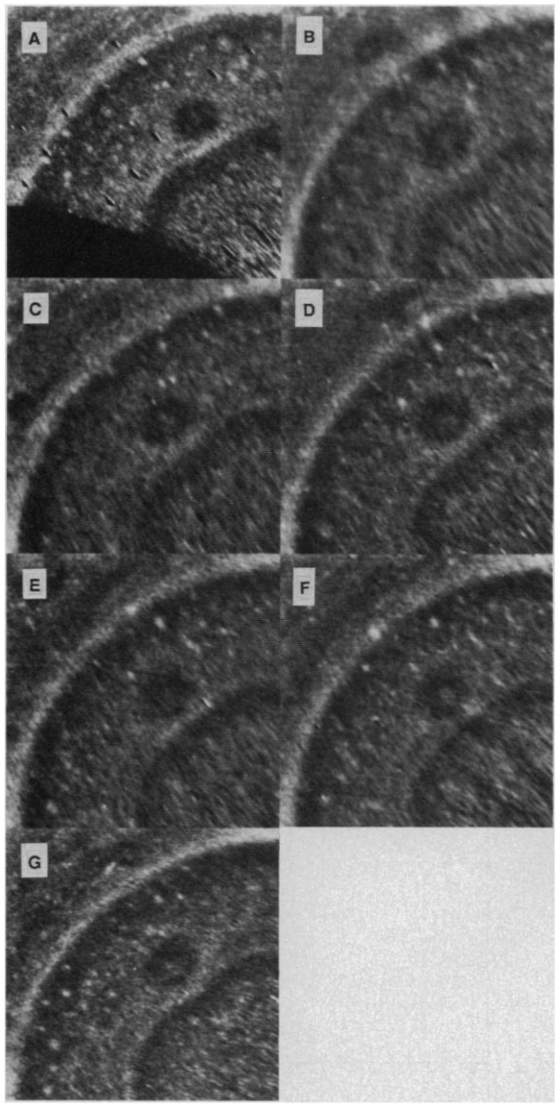

Fig. 1. A series of map projections showing how one quadrant of the hexagonal pattern around Saturn's north pole (and its associated spot) evolves with time: (**A**) a Voyager 1 image; (**B**–**G**) Voyager 2 images. There is a gap of 271 days separating the Voyager 1 image from the first Voyager 2 image. The Voyager 2 images cover a period of about 10 days. Thus it is unlikely that the scatter of these points is due to a regular longitude variation like that of Jupiter's Great Red Spot, which has a period of about 90 days (*6*).

Table 1. The variation in the position of the center (λ_c and λ_c') of the spot, as a function of time.

Image	Δt ($\times 10^7$ s)	λ_c (deg)	λ_c' (deg)
Fig. 1A	0.0	331.17	331.75
Fig. 1B	2.348	320.33	320.92
Fig. 1C	2.363	319.33	318.50
Fig. 1D	2.379	319.67	320.08
Fig. 1E	2.382	319.67	319.17
Fig. 1F	2.39	320.33	319.08
Fig. 1G	2.44	321.00	322.75

Table 2. The results of fitting a straight line to the values of λ_c and λ_c' given in Table 1. The χ^2 values use the errors resulting from the "0° offset" fit. Therefore, only their relative values are significant [$\chi^2 \propto \Sigma(y - y_i)^2$, where y represents the estimated value and y_i are the measurements]. The errors quoted are $\pm 1\sigma$.

Position	Offset (deg)	χ^2	Rotation rate $\times 10^{-9}$ rad s^{-1}	Rotation rate mm s^{-1}
λ_c	0	2.5	-8.13 ± 0.6	108 ± 7
	+360	1559	-271.5 ± 0.2	3598 ± 3
	−360	980	255.2 ± 0.2	-3382 ± 3
λ_c'	0	14	-8.5 ± 1.3	113 ± 17
	+360	1980	-271.8 ± 0.2	3602 ± 3
	−360	812	254.8 ± 0.2	-3377 ± 3

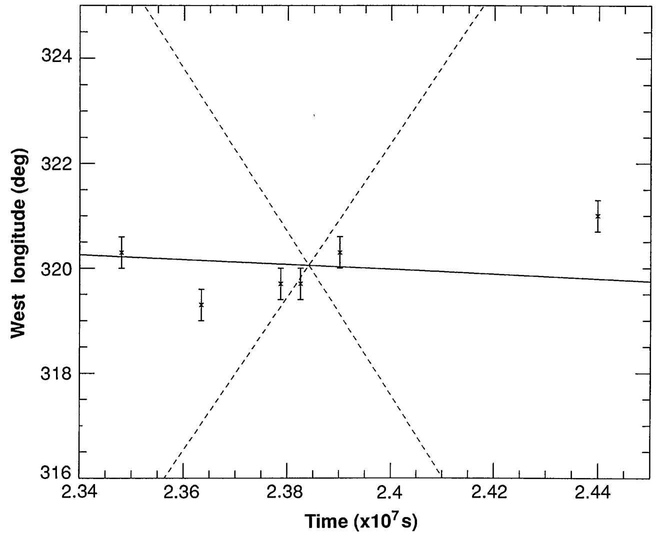

Fig. 3. An enlargement of part of Fig. 2. The dashed lines show how the fit changes if 360° is added to or subtracted from the position of the first point.

It is also clear from Fig. 1, A through G, that there is no justification for using other than a straight line fit in Fig. 2, in view of the comparatively large systematic errors. Another important reason for assuming a constant velocity is that the majority of features measured on the outer planets have a motion that is predominantly zonal, varying little over periods of many years (*4*).

The position of the first point in Fig. 2 assumes that the feature has not traveled one or more times around the planet in the interval separating Fig. 1, A and B. To investigate this possibility, I added 360° to and subtracted 360° from the position of the spot in Fig. 1A. The results of these fits for λ_c are shown in Fig. 3 and summarized in Table 2 along with the results for the center position λ_c' estimated by averaging the eastward and westward limits.

It is apparent, both from Fig. 3 and from the χ^2 values given in Table 2, that it is unlikely that the spot traveled one or more times around the planet between the Voyager 1 and Voyager 2 encounters. Averaging the results for λ_c and λ_c' given in Table 2 gives a mean rotation rate of $-8.19 \pm 0.52 \times 10^{-9}$ rad s^{-1} for the spot shown in Fig. 1 and for the hexagonal feature with which it is associated (error limits here and following are ± 1 SE). At the latitude of the hexagonal feature, this corresponds to a velocity of $+109 \pm 6.9 \times 10^{-3}$ m s^{-1}. This is in marked contrast to the velocities of over 100 m s^{-1} of the clouds that make up the hexagon (*1*).

So far, the motion of the hexagonal feature has been calculated relative to the radio rotation period (*5*); these periods can, however, be combined to give an absolute rotation rate of $16378.635 \pm 0.052 \times 10^{-8}$ rad s^{-1}. This gives a rotation period of 38362.082 ± 0.122 s or, equivalently, 10 hours 39 min 22.082 ± 0.122 s for the polar hexagon.

The hexagonal feature is not the only wavelike feature that moves very slowly, if at all, relative to a planet's radio rotation period. Recent measurements of the horizontal temperature field of Jupiter (*2*, *3*) have shown an oscillatory structure that moves within ≈ 10 m s^{-1} of the Jovian radio rotation period (also derived from the periodic radio emissions), even in the equatorial region where the visible clouds are moving at about 100 m s^{-1}.

Thus this apparent link between "surface" features and the periodic radio emissions occurs on both Jupiter and Saturn. In the Saturnian case it is clear that what is being seen is a phase velocity and not a material velocity. It is uncertain if this also applies to the Jovian features.

The association of surface features with the radio rotation periods suggests a connection between the deep interior of Saturn and the visible cloud level. Possible mechanisms for this were suggested in (*1*, *2*). If, as the mounting evidence implies, this association between the period of surface features and the radio emissions is real, the rotation period derived here is also an improved estimate of the internal rotation rate.

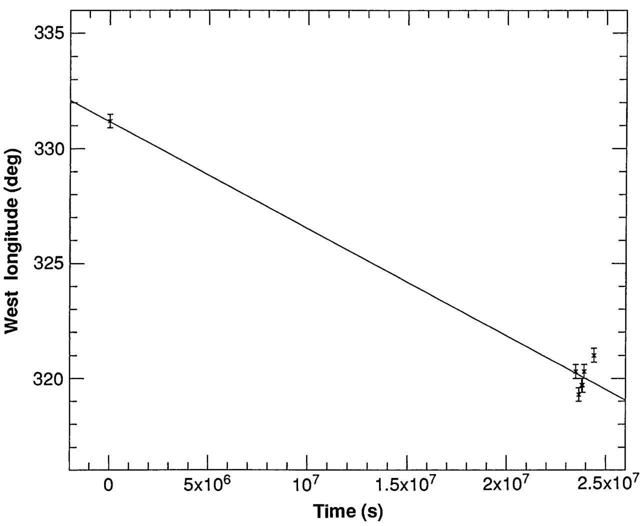

Fig. 2. Variation of the longitude of the large spot of Fig. 1 with time. The error bars show only the measurement error; other probable sources of error are described in the text.

REFERENCES AND NOTES

1. D. A. Godfrey, *Icarus* **76**, 335 (1988).
2. J. A. Magalhães *et al.*, *Nature* **337**, 444 (1989).
3. D. Deming *et al.*, *Astrophys. J.* **343**, 456 (1989).
4. A. P. Ingersoll, R. F. Beebe, B. J. Conrath, G. E. Hunt, in *Saturn*, T. Gehrels and M. S. Matthews, Eds. (Univ. of Arizona Press, Tucson, 1984), pp. 195–238.

5. M. D. Desch and M. L. Kaiser, *Geophys. Res. Lett.* **8** 253 (1981).
6. B. A. Smith and G. E. Hunt, in *Jupiter*, T. Gehrels, Ed. (Univ. of Arizona Press, Tucson, 1976), pp. 564–585.
7. I thank the National Space Science Data Center for supplying the data used in this study, which comes from the Voyager imaging experiments (team leader, B. A. Smith). I thank M. Belton and J. Christou for reading a draft version of this paper. The National Optical Astronomy Observatories are operated by the Association of Universities for Research in Astronomy, Inc., under contract to the National Science Foundation.

28 July 1989; accepted 16 January 1990

Steady-State Coupling of Ion-Channel Conformations to a Transmembrane Ion Gradient

EDWIN A. RICHARD AND CHRISTOPHER MILLER

Under stationary conditions, opening and closing of single *Torpedo* electroplax chloride channels show that the number of transitions per unit time between inactivated and conducting states are unequal in opposite directions. This asymmetry, which increases with transmembrane electrochemical gradient for the chloride ion, violates the principle of microscopic reversibility and thus demonstrates that the channel-gating process is not at thermodynamic equilibrium. The results imply that the channel's conformational states are coupled to the transmembrane electrochemical gradient of the chloride ion.

ION CHANNELS ARE A UBIQUITOUS class of integral membrane proteins that catalyze the passive diffusion of specific ions across biological membranes by forming hydrophilic pores. Channels can exist in nonconducting ("closed") and in ion-conducting ("open") conformations, whose interconversions may be driven by ligand binding, covalent modification, or electric fields. It is usually assumed that the opening and closing of ion channels represent conformational equilibria that are separate and distinct from the kinetic process of ions diffusing through the open pore. This study provides an example of an ion channel, the Cl^- channel from the electric organ of the electric ray *Torpedo californica*, whose individual transitions among conducting and nonconducting states display a strong asymmetry in time at the single-channel level and hence are not at equilibrium. Under our experimental conditions, the only free energy sources available for keeping the system away from equilibrium are transmembrane electrochemical gradients of aqueous solutes.

The Cl^- channel of *Torpedo* electroplax is unusual in that it operates by a "double-barreled shotgun" mechanism (*1, 2*). The channel complex is made up of two Cl^- diffusion pathways or "protochannels," which open and close independently of one another on the millisecond time scale. This behavior is apparent in the single-channel record shown in Fig. 1A; the channel displays three short-lived conductance levels, labeled U, M, and D, which represent states in which 2, 1, or 0 protochannels are open, respectively. An "inactivated" state, labeled I, is also apparent as long-lived nonconducting intervals (hundreds of milliseconds) separating bursts of rapid transitions between U, M, and D. This inactivated state is the result of a conformational change that shuts both protochannels simultaneously; bursts of channel activity occur when the channel complex leaves this inactivated state (*2*).

The traces in Fig. 1B show at a higher time resolution the seven inactivated periods displayed in the top trace. These events reveal a remarkable property of the transitions into and out of the I state: a high degree of asymmetry. In six of these seven cases, the channel entered the I state from M but left the I state into U. In 63 inactivated episodes, 31 were M→I→U and 1 was U→I→M. The remaining inactivated intervals were symmetrical: 29 M→I→M and 2 U→I→U.

To clarify the fundamental meaning of these observations, we should consider the directly observable transitions among U, M, and I. Records as in Fig. 1 show that this channel gates according to the following cyclic scheme, in which each state directly communicates with the other two:

$$\begin{tikzcd} & I \arrow[dl, shift left] \arrow[dr, shift left] & \\ M \arrow[ur, shift left] \arrow[rr, shift left] & & U \arrow[ul, shift left] \arrow[ll, shift left] \end{tikzcd}$$

The excess of M→I→U over U→I→M transitions means that the forward and backward rates of interconversions between the pairs of adjacent states U/I and M/I are unequal. This time asymmetry shows that detailed balance does not hold here and that therefore the three conformational states are not at thermodynamic equilibrium. Instead, they are maintained in a cyclic steady state in which net "clockwise" movement occurs around the state diagram. The maintenance of any reaction in a steady state always requires the input of external energy to keep the system away from equilibrium (*3*).

In these single-channel experiments, the individual conformational histories of single-channel molecules are observed directly. Therefore, the fluxes around the cycle in each direction, J_+ and J_-, could be measured directly from the channel record as the number of M→I→U→M and U→I→M→U cycles per unit time. It can be readily shown (*3*) on general thermodynamic grounds that the "asymmetry ratio," defined as the ratio of these unidirectional

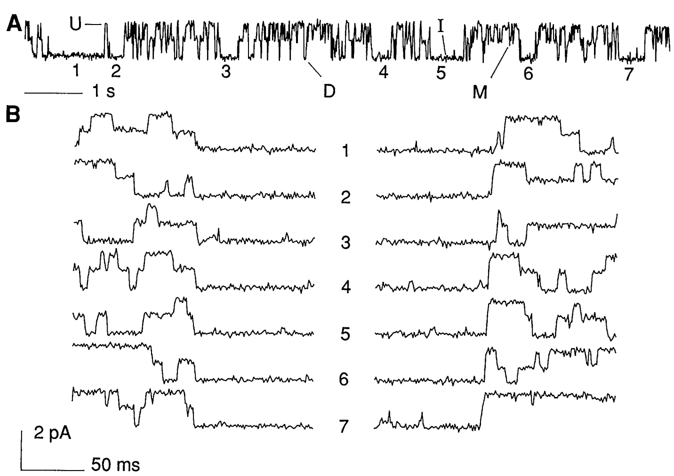

Fig. 1. Time asymmetry of a single *Torpedo* electroplax Cl^- channel. (**A**) A single-channel record at a slow time scale, with the four states of the channel labeled (U, D, M, and I), and the seven inactivated intervals numbered. (**B**) The same trace at an expanded time scale. Only the beginning and end of each inactivated state is shown, to allow identification of the states immediately preceding and following the inactivated interval. Single Cl^- channels were isolated by patch-recording from a planar bilayer (*9*) containing *Torpedo* Cl^- channels (*2*). All solutions used contained 1 m*M* $CaCl_2$, 0.1 m*M* EDTA, 150 m*M* KCl, and 10 m*M* Mops (4-morpholine propanesulfonic acid), *p*H 7.4. Voltage was held at −80 mV on the "cis" side, to which the *Torpedo* vesicles were added.

Howard Hughes Medical Institute, Graduate Department of Biochemistry, Brandeis University, Waltham, MA 02254.